Supplementary Information
for

Eutectic salt mixture-assisted sodium-vapor-induced synthesis of Pt−Ca nanoparticles, and their microstructural and electrocatalytic properties

Hiroshi Itahara*, Naoko Takahashi, Satoru Kosaka, Yasuhiro Takatani, Masanori Inaba, and Yuji Kamitaka

Toyota Central Research & Development Labs., Inc., 41-1 Yokomichi Nagakute, Aichi 480-1192, Japan, E-mail: h-itahara@mosk.tytlabs.co.jp

(1) Synthesis procedures

Pt nanoparticles supported on carbon powder (Pt/C; Tanaka Kikinzoku Kogyo K.K., TEC10V30E, [Pt] = 29.0 wt%) were used as the Pt source. The Pt/C powder was dispersed in a $CaCl_2$ aqueous solution, and then water was removed from the dispersion solution using an evaporator. The impregnation-prepared mixture powder of Pt/C and $CaCl_2$ (molar ratio of Pt:$CaCl_2$ = 1:1) was heat treated at 573 K under flowing Ar (500 mL/min) to remove residual water on the carbon surface.
[PtCa–H_2 sample] The mixture powder of Pt/C and $CaCl_2$ was heat treated at 873 K for 2 h under a H_2 gas (4 vol%/Ar balance) flow.
[PtCa–Na sample] The mixture powder of Pt/C and $CaCl_2$ was packed into a boron nitride (BN) crucible and a Na ingot was placed in another BN crucible (molar ratio of Pt:$CaCl_2$:Na = 1:1:2, total amount ~65 mg). These BN crucibles were then placed together in a stainless-steel cell (~10 cm^3 inner volume) so that the produced Na vapor contacted the powder mixture only when heated (873 K, 2 h). All procedures were conducted under an Ar atmosphere.
[PtCa–NaCl–Na sample] The mixture powder of Pt/C, $CaCl_2$, and NaCl (molar ratio of Pt:$CaCl_2$:$NaCl_2$ = 1:1:1) was prepared by the impregnation method. The powder was heated in Na vapor in the same manner described above (molar ratio of $CaCl_2$:Na = 1:2). After the heat treatment, all samples were washed using water to remove the unreacted salts and byproducts.

[PtMg–873K and PtMg–1173K samples] A mixture powder of Pt/C, $MgCl_2$, and NaCl (molar ratio of Pt:$MgCl_2$:$NaCl_2$ = 1:1:1) was prepared by the impregnation method. The powder was heated in Na vapor at 873 or 1173 K in the same manner described above (molar ratio of $MgCl_2$:Na = 1:2). The product powder was washed with water.

[PtSr–1173K sample] The mixture powder of Pt/C, $SrCl_2$, and NaCl (molar ratio of Pt:$SrCl_2$:$NaCl_2$ = 1:1:1) was prepared by the impregnation method. The powder was heated in Na vapor at 1173 K in the same manner described above (molar ratio of $SrCl_2$:Na = 1:2). The product powder was washed with 0.1 M HNO_3 aqueous solution.

(2) Synthesis and characterization of reference samples

(2-1) Comparison of the components in the samples before and after washing

As shown in Fig. S1 (a), the powder X-ray diffraction (XRD; Rigaku RINT-TTR) pattern of PtCa–Na samples before washing was assigned to $CaCl_2$, NaCl, Pt and Pt_2Ca. The peaks for $CaCl_2$ and NaCl were not detected for the XRD pattern of PtCa-Na sample after washing with water (Fig. S1 (b)).

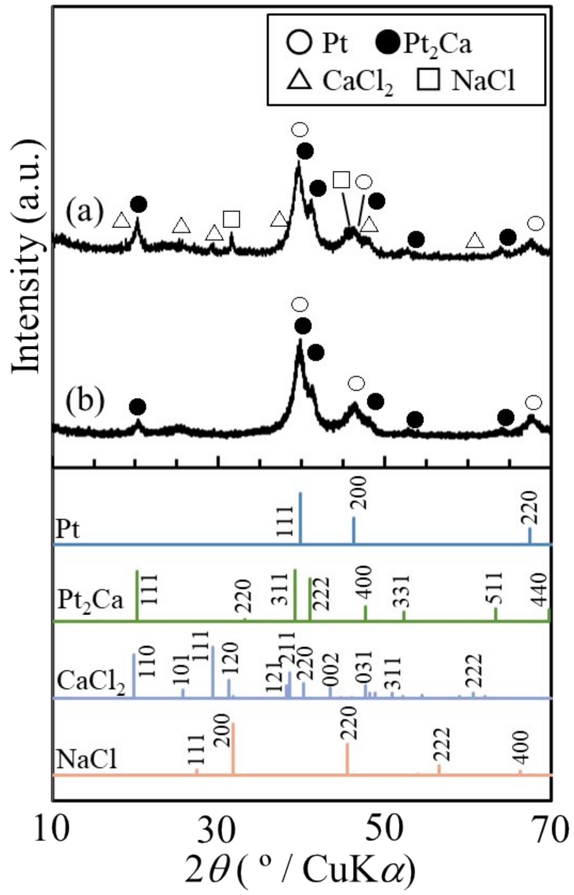

Figure S1. Powder XRD patterns for the PtCa−Na samples (a) before and (b) after washing with water. JCPDS Nos.: Pt (00-004-0802), Pt_2Ca (04-007-5045), $CaCl_2$ (00-024-0223) and NaCl (98-000-0235).

(2-2) Heat-treatment without Na vapor in Ar atmosphere

In order to consider the effect of Na vapor, the impregnation-prepared powder mixtures were heat treated at 873 K for 2 h without Na vapor in Ar atmosphere as a reference. The powder used was the mixture of Pt/C and $CaCl_2$ (molar ratio of Pt:$CaCl_2$=1:1) and the mixture of Pt/C, $CaCl_2$ and NaCl (molar ratio of Pt:$CaCl_2$:$NaCl_2$=1:1:1). For both samples, XRD peaks for Pt was sharpened when compared to those of the raw Pt/C powder while no Pt−Ca intermetallic phases were detected as shown in Fig. S2.

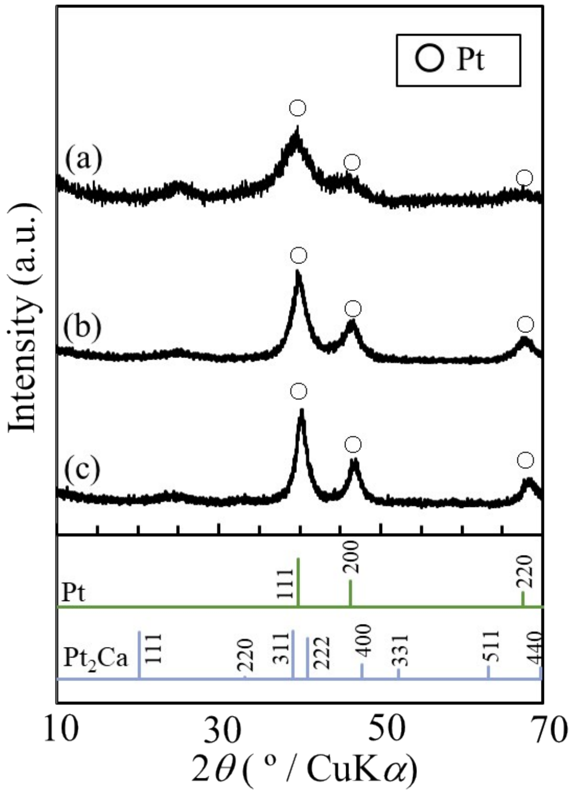

Figure S2. Powder XRD patterns for (a) raw Pt/C and samples obtained by heating (b) Pt/C+$CaCl_2$ powder and (c) Pt/C+$CaCl_2$+NaCl powder without Na vapor (after washing with water). JCPDS Nos.: Pt (00-004-0802) and Pt_2Ca (04-007-5045).

(2-3) Effect of synthetic temperatures

For the PtCa−Na sample, synthetic temperatures were set at 873 and 1173 K. XRD patterns shown in Fig. S3 suggests that the higher amount of Pt_2Ca was formed at higher synthetic temperature.

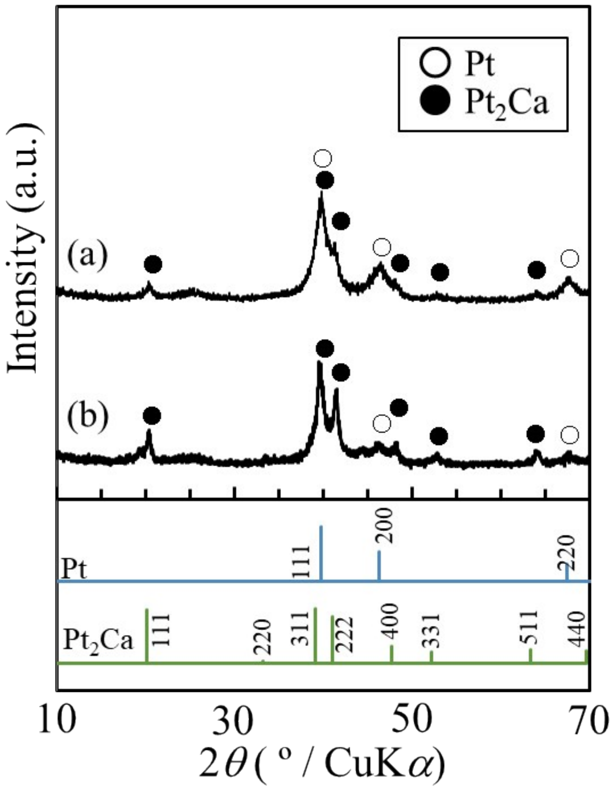

Figure S3. Powder XRD patterns of (a) PtCa−Na (873K) and (b) PtCa−Na (1173K) samples after washing with water. JCPDS Nos.: Pt (00-004-0802) and Pt_2Ca (04-007-5045).

(3) TEM images for PtCa−NaCl−Na sample

The particles with diameter of ca. 4-10 nm were observed (the round black contrasts) in transmission electron microscopy (TEM) images as shown in Fig. S4. The particles were supported on carbon (gray background contrast) with high loading amount and high dispersity.
STEM-EDX (scanning TEM energy dispersive X-ray spectroscopy; Thermo Fisher Scientific Inc. Talos F200X) was also conducted to identify the compositional distributions as shown in Fig.2 in the main text.

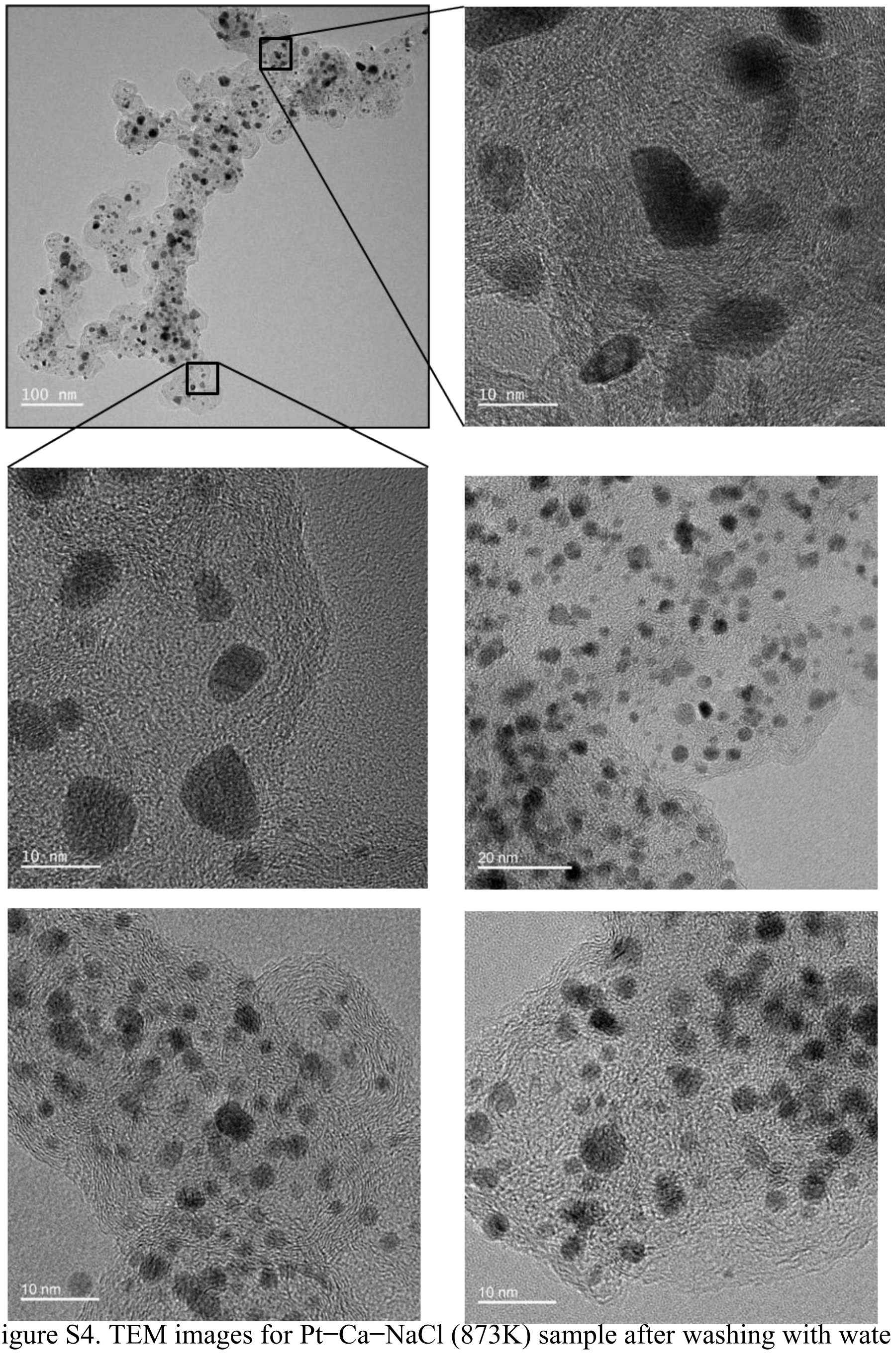

Figure S4. TEM images for Pt−Ca−NaCl (873K) sample after washing with water.

(4) SEM images for raw Pt/C

Figure S5 shows back scattered electron (BSE)-SEM (Hitachi High-Tech Co., S-5500) image. Pt nanoparticles (bright contrast) with a diameter of about 3 nm were highly dispersed on carbon (gray background) for the raw Pt/C powder. Crystallite size of Pt was 2.8 nm (see, XRD patten shown in Fig.S2(a)).

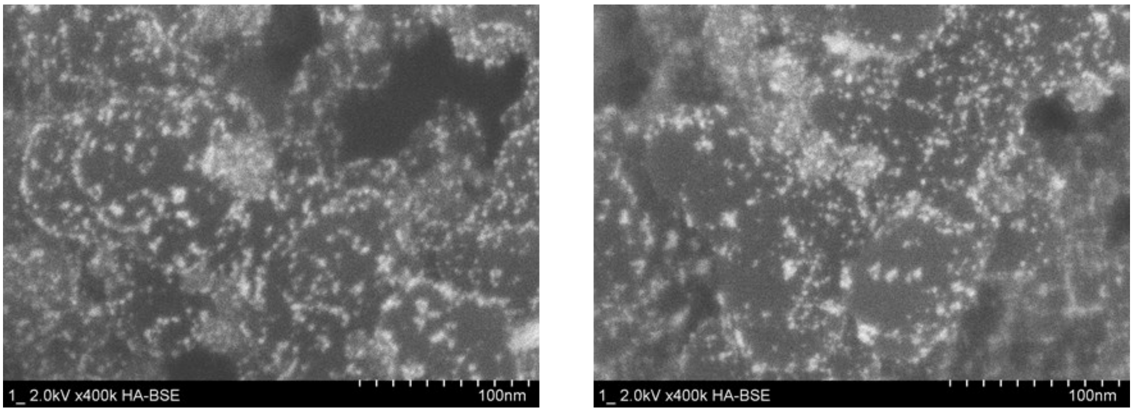

Figure S5. BSE-SEM images for raw Pt/C.

(5) STEM image and fast Fourier transform pattern for PtCa–NaCl–Na sample

Figure S6(a) shows a high-angle annular dark-field scanning TEM (HAADF-STEM; Thermo Fisher Scientific, Talos F200X) image of a particle in the PtCa–NaCl–Na sample. The Fourier transform pattern was indexed to the crystal structure of Pt_2Ca (*Fd*-3*m*, a = 0.7617 nm, $\alpha = \beta = \gamma = 90°$), as shown in Figs. S6(b) and 6(c). The structure is the same as that for the Pt_2Ca phase observed in the XRD pattern (JCPDS No. 04-007-5045) in Fig. 1(c) in the main text.
The pattern could not be indexed to the crystal structures of the other Pt–Ca intermetallic phases of Pt_2Ca ($P6_3/mmc$, $a = b$ = 0.5373 nm, c = 0.93110 nm, $\alpha = \beta = 90°$, $\gamma = 120°$), Pt_2Ca_3 (*R*-3, $a = b$ = 0.8786 nm, c = 1.6786 nm, $\alpha = \beta = 90°$, $\gamma = 120°$), Pt_2Ca_5 (*C*2/*c*, a = 1.6154 nm, b = 0.6627 nm, c = 0.7662 nm, $\beta = 97.5°$), Pt_3Ca_5 (I4/mcm, $a = b$ = 1.1563 nm, c = 0.5753 nm, $\alpha = \beta = \gamma = 90°$), Pt_5Ca (P6/mmm, $a = b$ = 0.5322 nm, c = 0.4368 nm, $\alpha = \beta = 90°$, $\gamma = 120°$), and Pt (*Fm*-3*m*, a = 0.39231 nm, $\alpha = \beta = \gamma = 90°$).

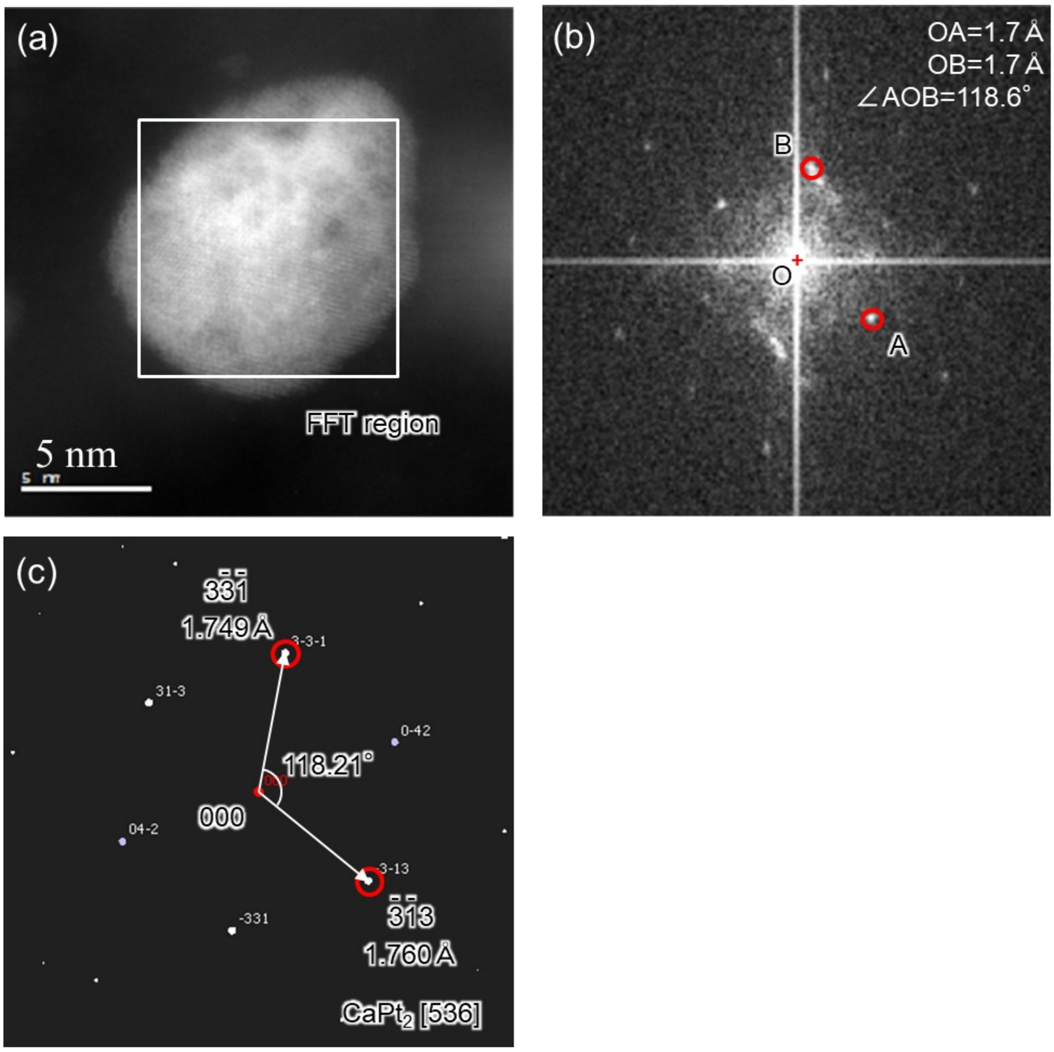

Figure S6. (a) STEM image for PtCa−NaCl−Na sample, (b) Fast Fourier transform (FFT) pattern acquired at the location shown by the square in (a), and (c) simulated diffraction pattern for Pt_2Ca.

(6) XRD pattern and SEM images for raw Pt/C

As a reference sample, the heat-treated Pt/C powder was prepared by heating the raw Pt/C powder (Tanaka Kikinzoku Kogyo K.K., TEC10V30E, [Pt] = 29.0 wt%) at 1123 K for 2 h in Ar flow (500 ml/min).

The heat-treated Pt/C powder had Pt particles with a similar diameter with Pt–Ca nanoparticles in the PtCa−NaCl−Na sample (Fig. S7(b) (XRD pattern, crystallite size: 5.2 nm) and Fig. S8 (BSE-SEM image, Pt: bright contrast, carbon: grey background)).

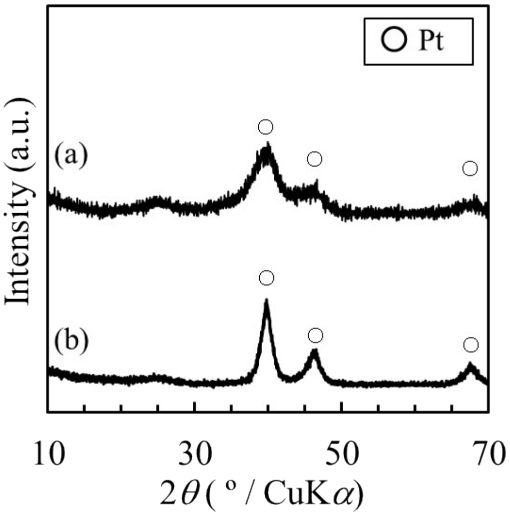

Figure.S7. Powder XRD patterns of (a) raw Pt/C and (b) heat-treated Pt/C (1123K) samples.

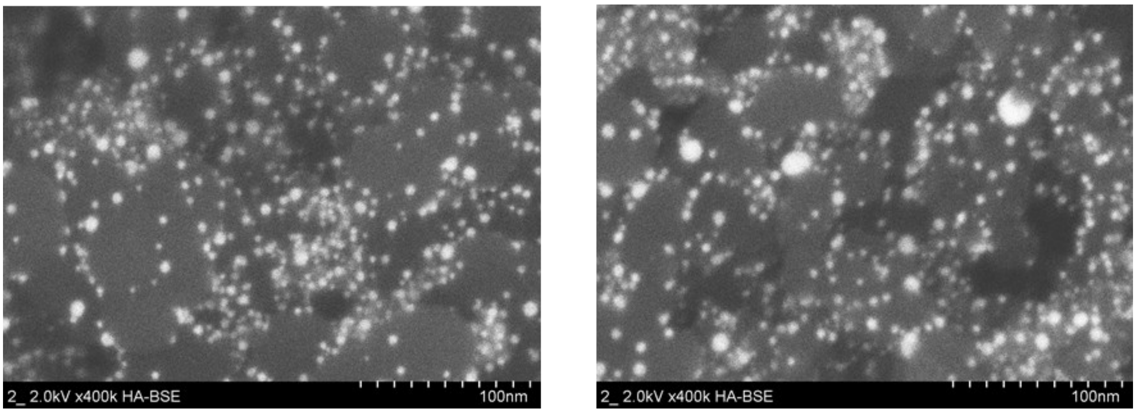

Figure S8. BSE-SEM images for heat-treated Pt/C (1123K) sample.

(7) Measurement conditions for chemical states of Pt and Ca

< X-ray photoelectron spectroscopy (XPS)>

XPS (PHI-5500MC, Ulvac Phi) measurements were conducted with Mg Kα X-rays at 1253.6 eV, 15 kV and 400 W. The base pressure was set to be less than 1×10^{-8} Pa. The diameter of detection was approximately 800 µm, and the take-off angle (TOA) was 45°. Here, the surface normal corresponds to a TOA of 90°. The pass energy and the energy step were set at 29.35 eV and 0.125 eV, respectively.

< hard X-ray photoelectron spectroscopy (HAXPES)>

HAXPES measurements were conducted at the BL16XU beamline of SPring-8. The photon energy was set at 7948 eV. The photoelectrons were assessed using a hemispherical analyzer (Scienta R4000).

The overall stability of the photoelectron energy was within 50 meV. The photoelectrons were determined at photoelectron TOA of 80°. Here, the angle perpendicular to the surface is defined as 90°.

< near-edge X-ray absorption fine structure (NEXAFS)>

NEXAFS spectra were measured at the BL6N1 beamline of the Aichi Synchrotron Radiation Center. During this measurement, photons from a storage ring (1.2 GeV) were monochromatized using Si(111) crystals, samples were loaded on In foil under Argon or air atmosphere and the spectra were collected in conversion electron yield and fluorescence yield modes under Helium atmosphere at an angle of incidence of $\theta = 20°$.

(8) Eextended X-ray absorption fine structure (EXAFS) and XANES (X-ray absorption near edge structure)

Pt L_{III}-edge XANES and EXAFS spectra (Fig. S9) were taken in the transmission mode using the BL16B2 beamline at SPring-8. The samples are the synthetic PtCa−NaCl−Na (Pt–Ca/C) sample and reference samples of Pt foil and Pt/C-HT (HT: heat-treated at 1123 K in Ar atmosphere). The Fourier transform (F.T.) was done in the *k*-range of 3-14 and *k*-weight of 3. It indicated the radial-structure function of the Pt atoms.

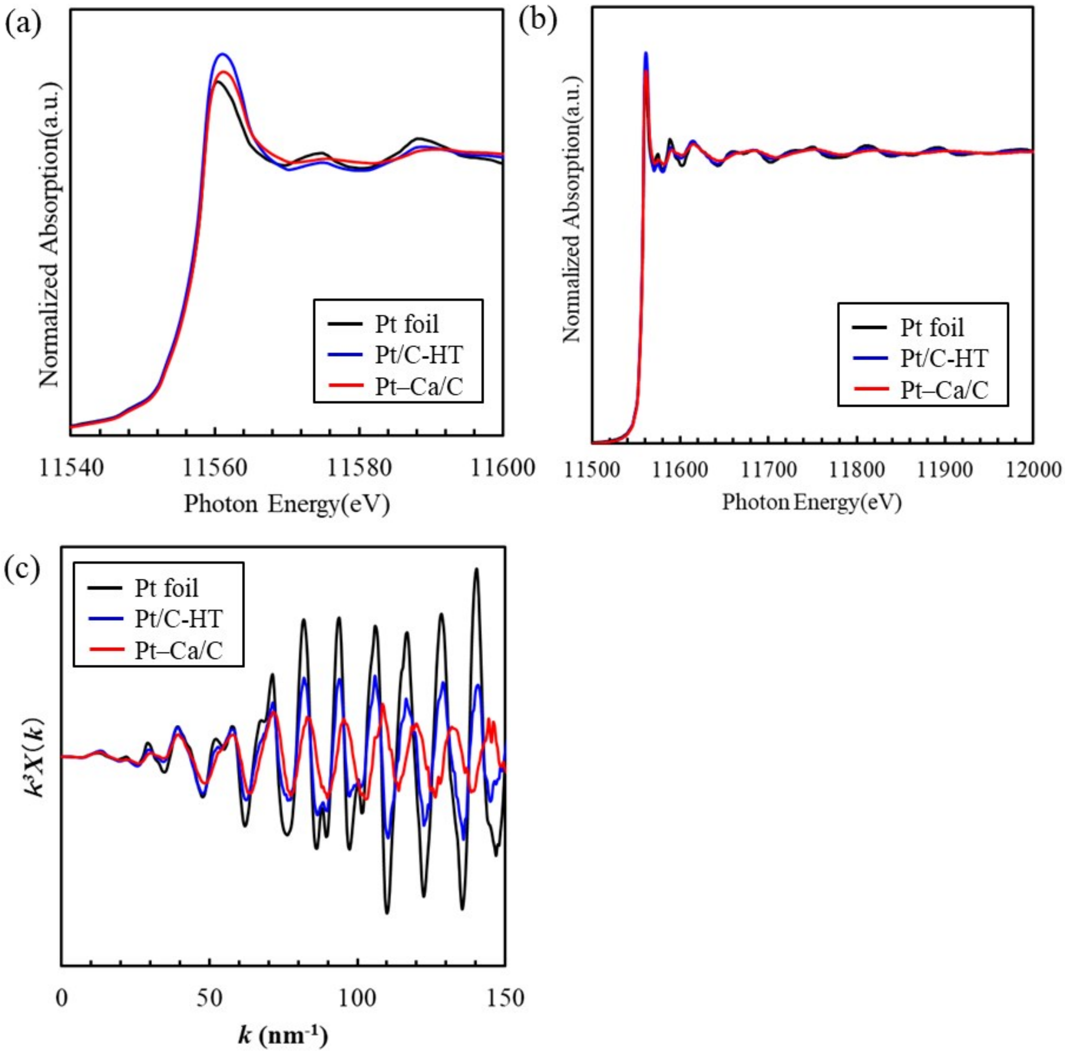

Figure S9. (a) XANES and (b)(c) EXAFS spectra.

(9) Catalytic activity evaluation of oxygen reduction reaction (ORR)

Catalyst inks were prepared by dispersion of PtCa−NaCl−Na or heat-treated Pt/C sample powers in ethanol and Milli-Q water (8:2 v/v) with Nafion (1 wt%) aqueous solution. The ink concentration was adjusted to 1 μg catalyst (*i.e.*, Pt_2Ca or Pt) in 5 μL of the ink and the weight ratio of Nafion and carbon was set to 0.1. The inks were ultrasonicated for ca. 45 min to yield uniform dispersions. About 1.5 μg catalyst (*i.e.*, Pt_2Ca or Pt) placed onto a glassy carbon electrode (5 mm in diameter) by using a spray coating method [1].

Electrochemical measurements were conducted using a general rotating-disk electrode technique [2-3]. A standard three-electrode cell was used for rotating disk electrode (RDE) measurements with Au mesh as a counter electrode and a reversible hydrogen electrode (RHE) as the reference electrode. The electrolyte was 0.1 M $HClO_4$ solution, prepared by diluting high-purity reagent $HClO_4$ (Kanto Chemical Co. Inc.) with Milli-Q water.

The catalyst-coated carbon electrode was first cycled in an Ar-saturated electrolyte between 0.05 and 1.2 V at a scan rate of 500 mV/s until a stable and reproducible cyclic voltammogram was obtained. In the current study, the following measurements were conducted after 500 cyclic voltammetry (CV) cycles at 500 mV/s.

The electrochemically active surface area (ECSA) was derived using the cyclic voltammogram recorded at 50 mV/s. The ECSA was estimated from the hydrogen adsorption/desorption peaks (H_{UPD}, observed at approximately 0.05–0.40 V) with subtraction of the double-layer capacitance (DLC_P, observed at approximately 0.40–0.60 V); the average H_{UPD} charge integrated for adsorption and desorption peaks (schematically shown in Fig. S10(a)) and a specific charge of $210\ \mu C/cm^2_{Pt}$ [4] were assumed.

Oxygen reduction reaction (ORR) curves (liner sweep voltammograms, LSVs) were recorded from 0.05 to 1.0 V at a scan rate of 10 mV/s in O_2-saturated electrolyte. During the measurements, the catalyst-coated carbon electrode was rotated at 1600 rpm. The kinetic current i_k at 0.9 V was determined from the Koutecký-Levich equation [2] of $1/i_k = 1/i - 1/i_d$ where i is the measured raw current at 0.9V and i_d is the O_2 diffusion limiting current. The ORR specific activity (SA) was calculated from i_k and ECSA. The mass activity (MA) was calculated from SA and the weight of catalyst used.

Here, theoretical i_d is expressed as $i_d = 0.62\ nFD^{2/3}w^{1/2}n^{-1/6}C^*$

n: number of electrons involved in the ORR
F: Faraday constant (96,485 C/mol)
D: diffusion coefficient of oxygen (2×10^{-5} cm^2/s for aqueous electrolyte at room temperature)
w: angular rotation rate of the electrode
n: kinetic viscosity of the solution (0.009 cm^2/s for aqueous electrolyte at room temperature).
C^*: bulk concentration of oxygen (1.2×10^{-6} mol/cm^3)

The theoretical i_d is ~6 mA/cm^2 in the case of the four-electron ORR ($n = 4$) typically observed for Pt and the current measurement condition of w of 1600 rpm.

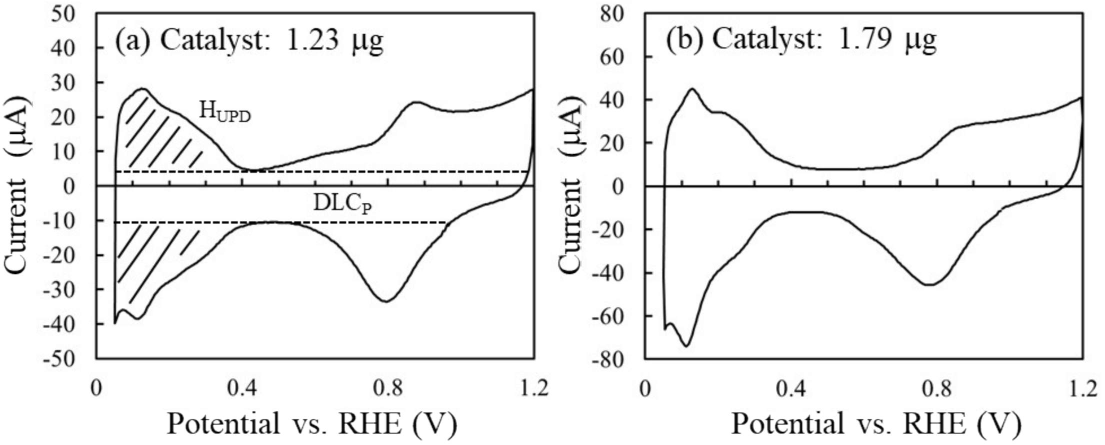

Figure S10. Cyclic voltammograms for (a) PtCa−NaCl−Na and (b) heat-treated Pt/C samples measured in the Ar-saturated 0.1 M $HClO_4$ solution at 50 mV/s. RHE represents the reference reversible hydrogen electrode.

(10) SEM images for the catalyst layer of Pt−Ca−NaCl (873K) sample before and after the electrochemical measurements.

No drastic morphological change was observed for the nanoparticles in PtCa–NaCl–Na sample after CV and ORR measurements under current evaluation conditions (Figs. S11 and S12, Pt–Ca: bright contrast, carbon: grey background). It is noted that a portion of small particles may not be clearly observed because the contrasts were weakened by Nafion covering the nanoparticles.

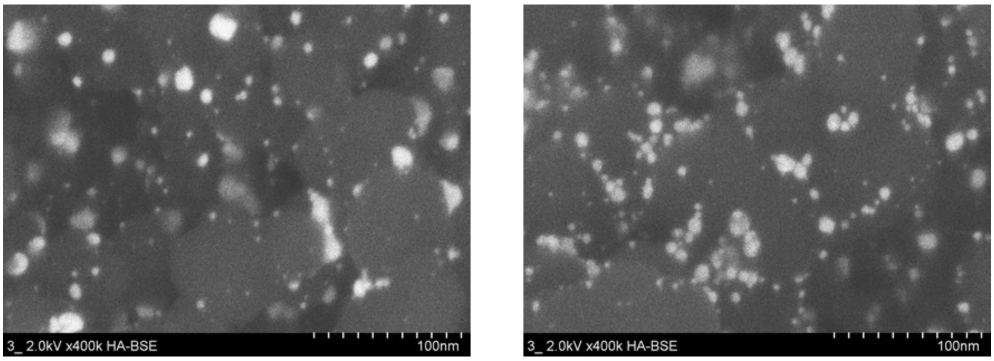

Figure S11. BSE-SEM images for the catalyst layer of Pt−Ca−NaCl (873K) sample before electrochemical measurements.

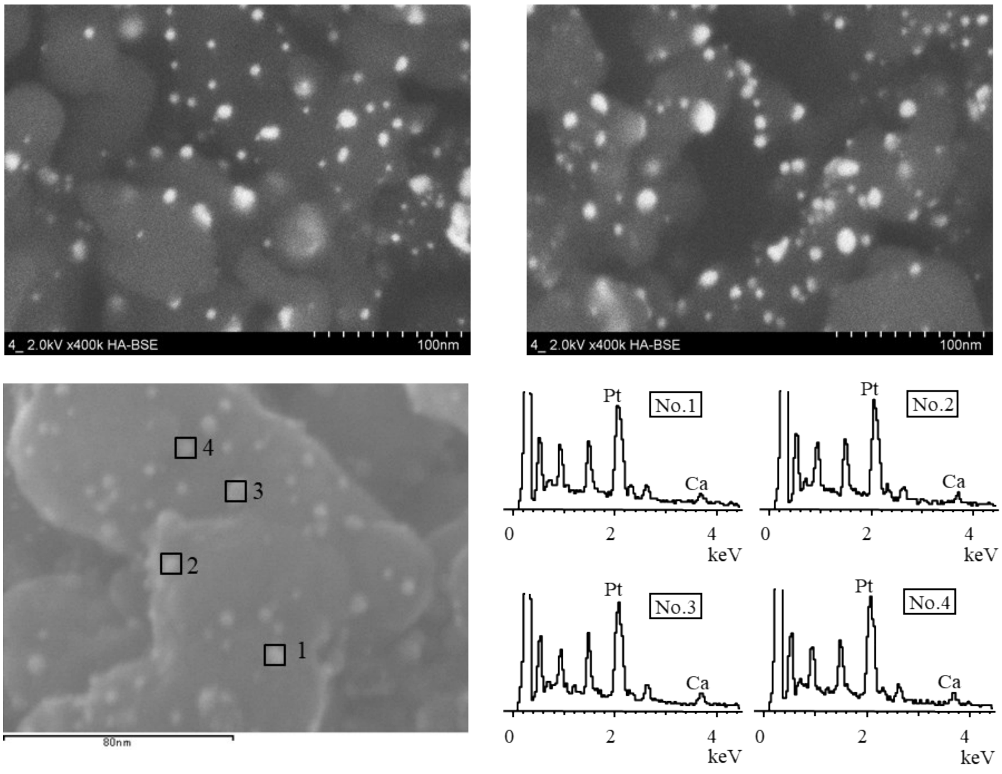

Figure S12. BSE-SEM images and EDX analysis for the catalyst layer of Pt−Ca−NaCl (873K) sample after electrochemical measurements.

References
(1) M. Inaba, Y. Kamitaka and K. Kodama, *J. Electroanal. Chem*. 2021, **886**, 115115.
(2) A. J. Bird and L. R. Faulkner, Electrochemical methods: Fundamentals and applications. 2nd ed., 2020, Jhon Wiley & Sons., New York.
(3) T. J. Schmidt, H. A. Gasterger, G. D. Stäb, P. M. Urban, D. M Kolb and R. J. Behm, *J. Elctrochem. Soc.*, 1998, **145**, 2354.
(4) S. Gilman, *J. Phys. Chem*., 1963, **67**, 78.